Journal of the European Ceramic Society 22 (2002) 689–696

www.elsevier.com/locate/jeurceramsoc

Space charge segregation during the cooling process and its effect on the grain boundary impedance in Nb-doped $BaTiO_3$

Seok Hyun Yoon, Hwan Kim*

School of Materials Science and Engineering, College of Engineering, Seoul National University, Seoul 151-742, South Korea

Received 11 January 2001; accepted 28 April 2001

Abstract

Highly donor-doped and large grained $BaTiO_3$ ceramics can be prepared by sintering in a reducing atmosphere. If these specimens are again heat treated at a certain sintering temperature and cooled in air, PTCR (positive temperature coefficient resistor) characteristics appear. When the cooling rate is low, another third RC (resistance-capacitance) component appears besides that of the grains and grain boundaries in impedance analysis. This RC component is associated with donor segregation. It is not observed when the cooling rate is high. In the slightly donor-doped specimens where the cooling rate, microstructure and R (resistivity)–T (temperature) properties are similar to the former, this third RC component also does not appear. The segregation related phenomena were confirmed by STEM/EDS analysis. These trends correspond to the space charge segregation theory that explains that the space charge potential, which acts as the driving force for donor segregation, becomes large during the cooling process in air.

Keywords: $BaTiO_3$; Grain boundaries; Impedance; PTC devices; Segregation

1. Introduction

There are many applications for donor-doped $BaTiO_3$ such as PTCR, boundary layer capacitors etc. As a result, this material has been intensively studied, especially for grain boundary phenomena, which determine the properties of these devices. Among the grain boundary phenomena observed, grain boundary segregation is crucial because it has a remarkable effect on both the electrical properties and microstructures. In the case of acceptor-doped $BaTiO_3$, acceptor segregation was easily detected, and there is ample experimental evidence.[1–4] As for donor-doped $BaTiO_3$, although donor segregation was not as easily detected as acceptor segregation,[1–2, 5] several researchers provided evidence of donor segregation in barium titanate through compositional analysis.[4,6–7]

However, it is not clear in these reports that mentioned donor segregation, whether donor segregation was caused by the driving force of the space charge potential or by misfit strain energy. Application of the space charge segregation theory to donor-doped $BaTiO_3$ explains that a high donor concentration, high oxygen partial pressure and low temperature favor donor segregation.[8] The magnitude of the space charge potential that causes the driving force for donor segregation increases as the cooling process proceeds from sintering temperature in air. Therefore, in order to verify that donor segregation in donor-doped $BaTiO_3$ is caused by the space charge potential, it should be shown that initially homogeneously distributed donors can segregate during the cooling process from sintering temperature in air.

When donor segregation occurs in the grain boundary region, it results in the formation of highly resistive layers at the grain boundary, by shifting the donor incorporation from electronic to vacancy compensation. Thus, the total resistivity of the sample can be represented by the grain resistance, the resistance from a potential barrier and the resistance from the dopant-segregation-induced insulating region.[9,10] Based on this model, the insulating layer may act as another R (resistance) C (capacitance) component that is different from the conventional PTCR (positive temperature coefficient

* Corresponding author. Tel.: +82-2-880-7158; fax: +82-2-884-1413.

E-mail addresses: hwkim@gong.snu.ac.kr (H. Kim), maniacaa@gong.snu.ac.kr (S. H. Yoon).

0955-2219/02/$ - see front matter
PII: S0955-2219(01)00305-3

resistor) equivalent circuit components of grains and grain boundaries. Recently a report presented indirect evidence for donor segregation and its effect on grain boundary impedance in $BaTiO_3$ by detecting the third RC component in impedance/modulus analysis.[8]

Generally above certain doping concentrations (about 0.4–0.5 mol%), donor-doped $BaTiO_3$ reverts to insulating behavior and its grain size becomes very small. However, if sintered in a reducing atmosphere, semiconducting specimens can be obtained with a large grain size and homogeneous donor distribution even though the donor concentration is high. In this study, these specimens were heat treated at a sintering temperature in air with different cooling rates, and the possibility of donor segregation was investigated. In slightly and heavily donor-doped specimens of which the microstructures and *R*(resistivity)-*T*(temperature) properties are similar to each other, differences in impedance data were analyzed. In addition, whether or not donor segregation occurs during the cooling process in air was confirmed by STEM (scanning transmission electron microscopy)/EDS (energy dispersive X-ray spectroscopy) analysis.

1.1. Experimental procedures

$BaTiO_3$ (Fuji-Titanium Industry Co., 99.8%), Nb_2O_5 (Aldrich Chemical Co., 99.9%), MgO (High Purity Chemicals, 99.98%), $BaCO_3$ (Aldrich Chemicals Co., 99.98%), MnO_2 (High Purity Chemicals, 99.99%) and TiO_2 (Aldrich Chemicals Co., 99.9%) powders were used as starting materials. Donor Nb and acceptor Mg or Mn were incorporated into the Ti sites substitutionally ($Nb_{Ti}^{\bullet}$, Mg_{Ti}'', and Mn_{Ti}' or Mn_{Ti}''). The compositions of the specimens in this study are listed in Table 1. The actual compositions were prepared by mixing undoped $BaTiO_3$, Nb_2O_5, MgO, and $BaCO_3$, and designed for unit A:B site ratio.

These donor and acceptor doped $BaTiO_3$ powders were ball milled with ethanol in a polypropylene jar for 24 h then dried and calcined at 1100°C for 2 h followed by additional ball milling. The resulting powders were pressed into disks and treated with cold isostatic pressing at a pressure of 150 MPa. 0.1 mol% Nb–0.05 mol% Mn-doped $BaTiO_3$ (slightly donor-doped) specimens were sintered at 1400°C for 2 h in air with a heating rate of 300°C/h and a cooling rate of 160°C/h to 900°C, and followed by furnace cooling. 0.85 mol% Nb-doped (heavily donor-doped) $BaTiO_3$ specimens were sintered at 1300°C for 2 h in a reducing atmosphere (oxygen partial pressure $PO_2 = 10^{-10}$ atm, CO/CO_2 atmosphere) then heat-treated at 1400°C for 2 h in air with a heating rate of 300°C/h and a cooling rate of 160°C/h and 800°C/h to 900°C respectively, and followed by furnace cooling.

In order to identify whether donor segregation in $BaTiO_3$ occurs during the cooling process in air or not, STEM/EDS analysis was performed. However, in the above concentration range it is very difficult to detect the segregation phenomenon unless severe segregation occurs. This is because in EDS analysis the peaks corresponding to atoms where the concentrations are 1–2 mol% are difficult to distinguish from the background noise. Thus, for STEM/EDS analysis, 6 mol% Nb–2.6 mol% Mg-doped $BaTiO_3$ (net 0.8 mol% Nb) specimens were sintered at 1300°C for 2 h in a reducing atmosphere ($PO_2 = 10^{-10}$ atm, CO/CO_2 atmosphere) then heat-treated at 1400°C for 2 h in air with a heating rate of 300°C/h and a cooling rate of 50°C/h to 900°C, followed by furnace cooling. The conditions for specimen preparation are listed in Table 1.

The electrodes for electrical property measurements were prepared by silk printing an In–Ga paste for ohmic contact and a Ag paste for the protecting electrodes. These were heat treated at 600°C for 30 min. The resistivities were measured using a DC method with a digital multimeter (3478A, Hewlett-Packard) in the temperature range of 30–300°C. Impedance data were measured by a LF impedance analyzer (HP4192, Hewlett-Pack-

Table 1
Conditions for specimen preparation

Composition	Heat treatment condition	Abbreviation
0.1 mol% Nb–0.05 mol% Mn-doped $BaTiO_3$ ($BaTi_{0.9985}Nb_{0.001}Mn_{0.0005}O_3$)	Sintering at 1400°C 2 h in air ($PO_2 = 0.2$ atm), cooling rate: 160°C/h	0.1Nb–0.05Mn–BT-160
0.85 mol% Nb-doped $BaTiO_3$ ($BaTi_{0.9915}Nb_{0.0085}O_3$)	Sintering at 1300°C 2 h in a reducing atmosphere ($PO_2 = 10^{-10}$ atm) ⇒ Heating at 1400°C 2 h in air Cooling rate: 160°C /h	0.85Nb–BT-160
	Sintering at 1300°C 2 h in a reducing atmosphere ($PO_2 = 10^{-10}$ atm) ⇒ Heating at 1400°C 2 h in air Cooling rate: 800°C /h	0.85Nb–BT-800
6 mol% Nb–2.6 mol% Mg-doped $BaTiO_3$ (net 0.8 mol% Nb) ($BaTi_{0.914}Nb_{0.06}Mg_{0.026}O_3$)	Sintering at 1300°C 2 h in a reducing atmosphere ($PO^2 = 10^{-10}$ atm) ⇒ Heating at 1400°C 2 h in air Cooling rate: 50°C /h	6Nb–2.6Mg–BT-50

ard) in the temperature range of 30–400°C. Evaluation of each RC component value for a properly assumed equivalent RC circuit and data analysis was carried out using EQUIVALENT CIRCUIT (Version 3.97) software which extracts R, C, and n (relaxational distribution parameter ranging from zero to unity) by non-linear least squares fitting.

Thermal etching was carried out at 1300°C for polished samples and the microstructures were observed using scanning electron microscopy (SEM, Jeol JSM 5600). The chemical compositions at the grain and grain boundaries were analyzed with STEM (Phillips CM20) with EDS attachment.

2. Results and discussions

Fig. 1(a) and (b) shows the microstructures of the 0.1 mol% Nb–0.05 mol% Mn-doped $BaTiO_3$ specimen sintered at 1400°C in air, and 0.85 mol% Nb-doped $BaTiO_3$ specimen sintered at 1300°C in a reducing atmosphere ($PO_2 = 10^{-10}$ atm), respectively. Both specimens have similar microstructures with average grain sizes of 40–50 μm. Thus, there is no possibility that the difference in electrical impedance data is due to differences in microstructures. Fleig et al. reported that there is the possibility of the occurrence of a third semicircle due to constriction resistance.[11] Very porous materials that show incomplete wetting of the grain surfaces or poor grain-to-grain contact can exhibit this phenomenon. Thus, if the specimen shown Fig. 1(a) has two RC components of grains and grain boundaries and the specimen shown Fig. 1(b) shows another third RC component in addition to the two, it can be expected that the third RC component is not due to constriction resistance, because the microstructures are the same in both cases.

Fig. 2 shows R (resistivity)–T (temperature) curves for 0.1Nb–0.05Mn–BT-160, 0.85Nb–BT-160 and 0.85Nb–BT-800 specimens. The room temperature resistivities of 0.85 mol% Nb-doped $BaTiO_3$ specimens are very sensitive to cooling rate after heat treatment in air, and were above 10^7 Ωcm insulating when the cooling rate was lower than 100°C/h in our experiment. In both 0.1Nb–0.05Mn–BT-160 and 0.85Nb–BT-160 specimens, R_{min} (minimum resistivity) and R_{max} (maximum resistivity) were similar to each other and were 10^4 Ωcm and over 5×10^7 Ωcm, respectively.

The magnitude of the theoretically derived space charge potential in the temperature range of 1000–1400°C that causes the driving force for donor segregation, is small for low PO_2 and high temperatures, and large for high PO_2 and low temperatures.[8] Near the sintering temperature, the equilibrium defect distributions in the grain boundary regions are maintained. However, as the cooling process proceeds, the equilibrium defect distributions corresponding to each decreasing temperature are not maintained due to kinetic problems. Thus, in the case of a high cooling rate, the donor distribution in the grain boundary region will be similar to the equilibrium donor distributions of high temperatures, and in the case of a low cooling rate, the donor distribution in the grain boundary region will be similar to the equilibrium donor distributions of lower temperatures. This means that a lower cooling rate enhances donor segregation. Thus, it is expected that donor segregation occurs far more in the 0.85Nb–BT-160 specimen than in the 0.85Nb–BT-800 specimen.

In the 0.1Nb–0.05Mn-BT specimen where net donor concentration is very low, the values of the space charge potential are small in the overall temperature range (1000–1400°C), and the increase in the values are negligible with decreasing temperature. Thus, donor segregation is not expected to occur.

The resistivity of the 0.1Nb–0.05Mn–BT-160 specimen is dominated by the grain boundary resistivity that is caused by grain boundary oxidation during the cooling process in air. However, the resistivity of the 0.85Nb–BT-160 specimen is dominated not only by the grain

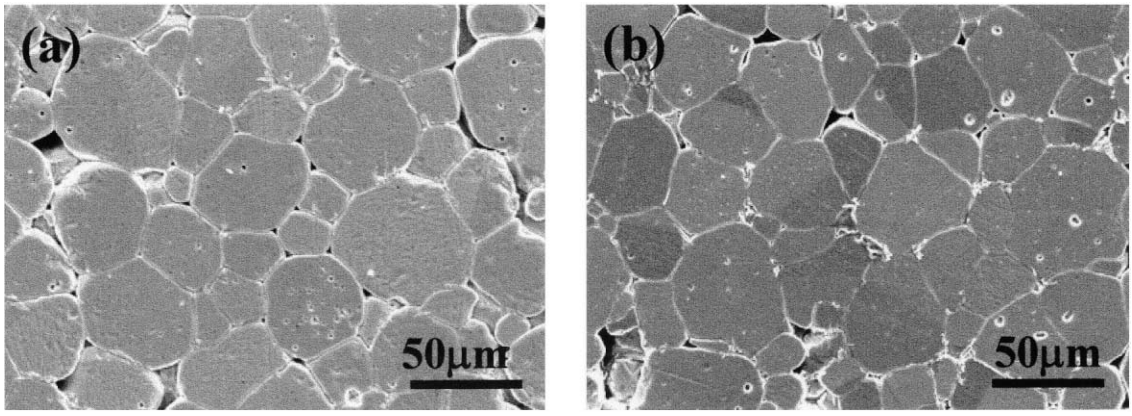

Fig. 1. Microstructures of (a) the 0.1 mol% Nb–0.05 mol% Mn-doped $BaTiO_3$ specimen that was sintered at 1400°C in air, and (b) the 0.85 mol% Nb-doped $BaTiO_3$ specimen that was sintered at 1300°C in a reducing atmosphere ($PO_2 = 10^{-10}$ atm).

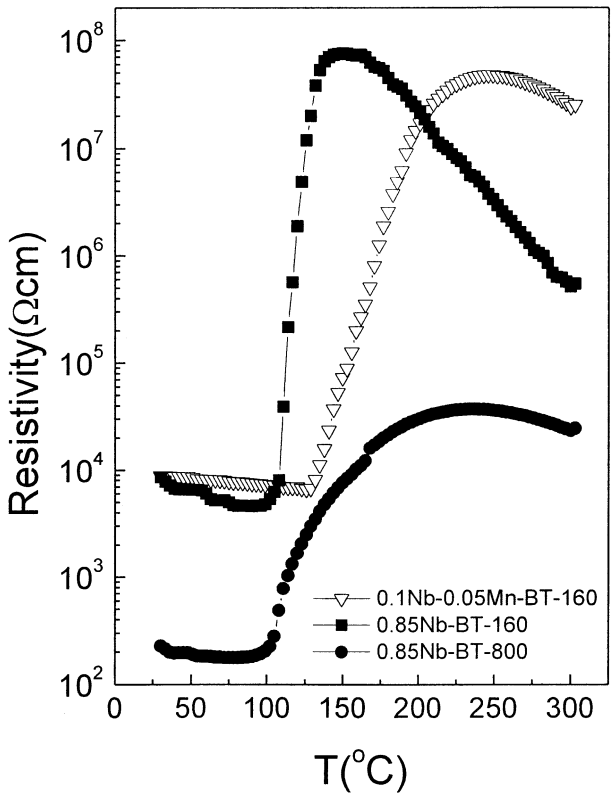

Fig. 2. *R* (resistivity)–*T* (temperature) curves for 0.1Nb–0.05Mn–BT-160, 0.85Nb–BT-160 and 0.85Nb–BT-800 specimens.

boundary resistivity, which is caused by grain boundary oxidation, but also by the resistivity that is caused by a segregation-induced insulating layer during the cooling process in air. Therefore, although the *R* (resistivity)–*T* (temperature) properties are similar between the two specimens, there may be differences in the RC components.

Fig. 3 shows the complex modulus plane plots of measured and fitted data for the 0.1Nb–0.05Mn–BT-160 specimen at different temperatures. In all temperature ranges the measured modulus data can be fitted to two RC responses, which means that the specimen is composed of two RC components. The semi-circle in the low frequency range is due to the grain boundary RC component, and that in the high frequency range is due to the grain core RC component. This behavior is identical to the conventional PTCR equivalent circuit model.

Fig. 4 shows the complex modulus plane plots of measured and fitted data for the 0.85Nb–BT-160 specimen at different temperatures. It appears that the modulus data at 100°C is described by two semicircles of which the one in the low frequency range is flat. The modulus data at 180°C also shows two semicircles. However the semicircle in the low frequency range does not start at the zero point. That is, the semicircle corresponding to the data below 50 Hz is completely cut off and is not shown. At 240°C, a hidden semicircle appears. The measured data can be

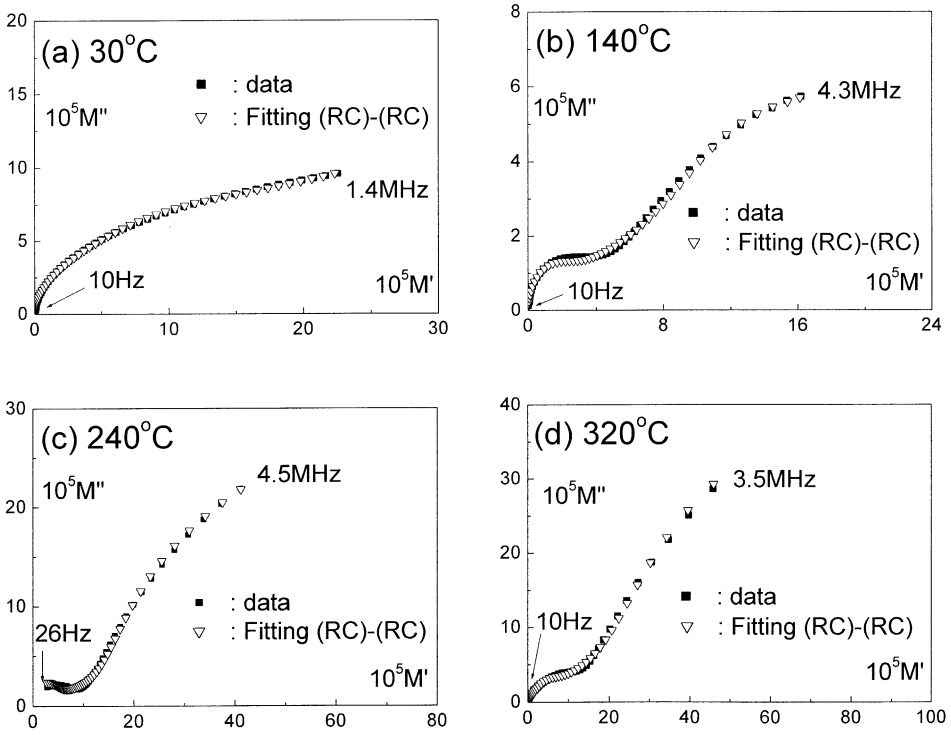

Fig. 3. Complex modulus plane plots of measured and fitted data for the 0.1Nb–0.05Mn–BT-160 specimen at different temperatures: (a) 30°C, (b) 140°C, (c) 240°C, (d) 320°C.

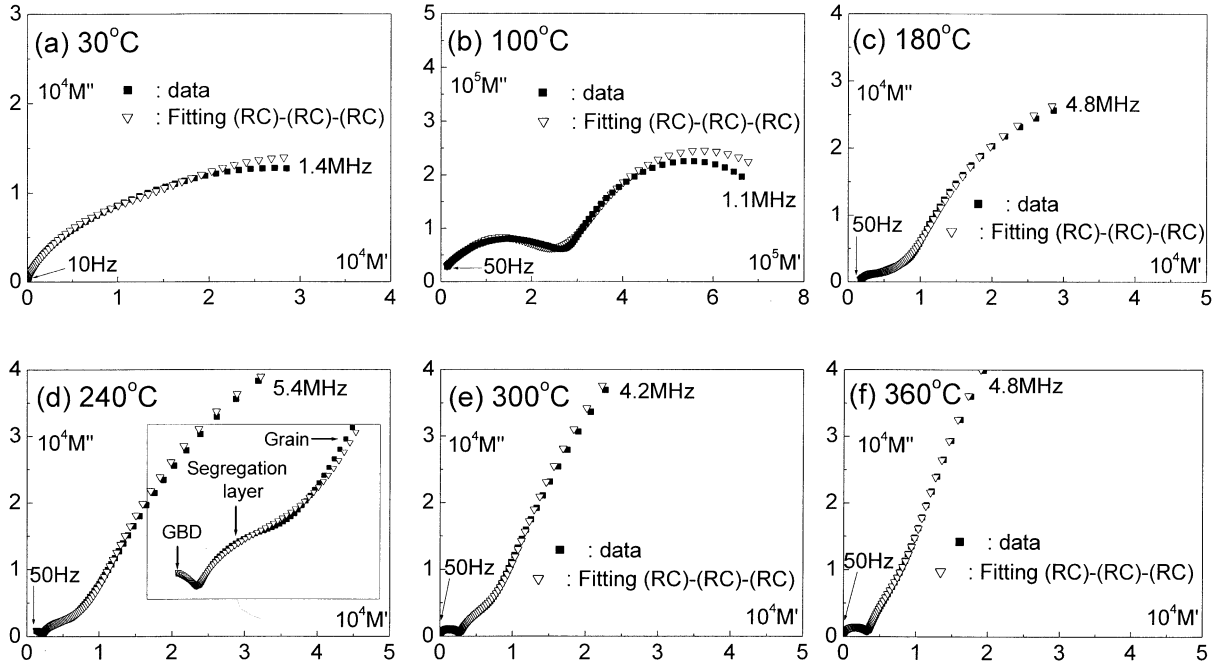

Fig. 4. Complex modulus plane plots of measured and fitted data for the 0.85Nb–BT-160 specimen at different temperatures: (a) 30°C, (b) 100°C, (c) 180°C, (d) 240°C, (e) 300°C, (f) 360°C.

fitted to three RC responses in all temperature ranges. Thus this specimen is composed of three RC components. The semicircle in the lowest frequency range is due to the grain boundary RC component, and that in the highest frequency range is due to the grain core RC component. The semicircle in the middle frequency range is associated with the RC component of the segregation-induced insulating layer. Near T_C, two semicircles corresponding to grain boundary and segregation layer are superimposed [Fig. 4(b)]. Also, as the temperature increases further, the semicircle corresponding to the segregation layer moves to a higher frequency range [Fig. 4(c)–(f)]. That is, the RC value of the segregation layer becomes increasingly similar to that of the grain from that of grain boundary with the increase of temperature. This third RC component begins to disappear above 360°C.

Fig. 5 shows the resistance values of each RC element of 0.85Nb–BT-160 specimen with temperature extracted from curve fitting. Resistance values of grain are roughly constant with temperature. Resistance values of grain boundary and segregation layer show PTCR effects, and NTCR (negative temperature coefficient resistor) effects above the PTCR maximum.

Fig. 6 shows reciprocal capacitance values of grain and grain boundary of the 0.85Nb–BT-160 specimen with temperature extracted from curve fitting. The capacitance data of grain follow the Curie–Weiss law. The capacitance data of grain boundary are roughly temperature independent at high temperatures, and a departure occurs in which reciprocal values of grain

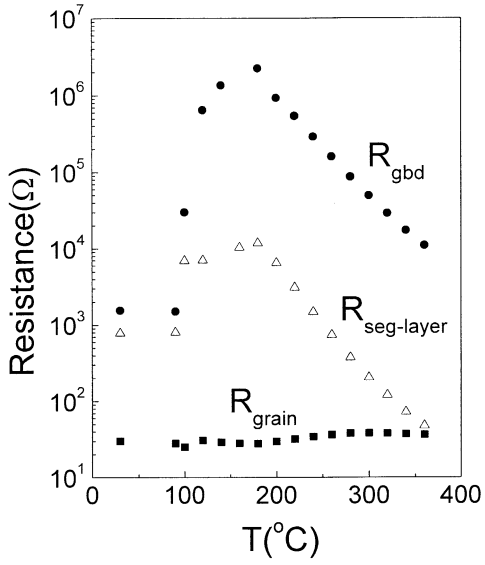

Fig. 5. Resistance values of each RC element of the 0.85Nb–BT-160 specimen with temperature extracted from curve fitting.

boundary (C_{gb}^{-1}) appear to decreases around the Curie temperature (T_C). This behavior is similar to the trend of the constriction boundary model.[12] The equivalent circuit and data analysis appear to be realistic, since the above resistance and capacitance values of each RC component extracted from the nonlinear least squares (NLLS) fitting method show simple and reasonable temperature dependence.

All these behaviors of each RC element of the 0.85Nb–BT-160 specimen are similar to those previously reported

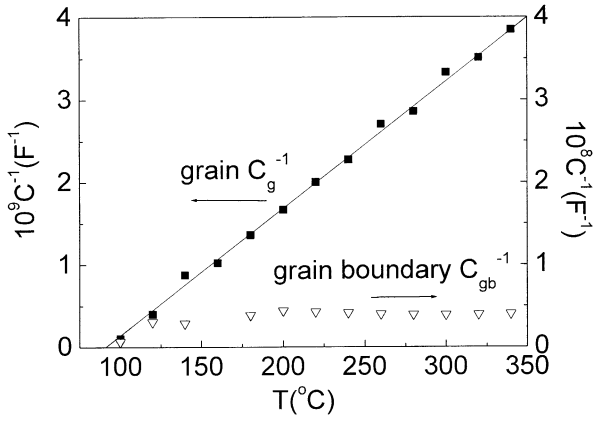

Fig. 6. Reciprocal capacitance values of grain and grain boundary of the 0.85Nb–BT-160 specimen with temperature extracted from curve fitting.

in the heavily donor-doped specimens (0.5 mol% Nb–0.07 mol% Mg-doped $BaTiO_3$) that were sintered in air, which were reported to be indirect evidence for donor segregation.[8] In the reports, the disappearance of the RC element associated with donor segregation above 360°C was explained by a Fermi level change in the dopant segregation layer with a change in temperature and the valence change of titanium vacancies from V_{Ti}'''' to V_{Ti}'''. Thus, it is expected that donor segregation has occurred in the 0.85Nb–BT-160 specimen.

Fig. 7 shows complex modulus plane plots of measured and fitted data for the 0.85Nb–BT-800 specimen at different temperatures. In all temperature ranges the measured modulus data can be fitted to the responses of one R (resistance) component and one RC component. One semicircle appears and this is due to the grain boundary RC component. The semicircle associated with the grain core RC component is outside the range of measuring frequency, or the grain core is represented by only the resistance component. Thus, in this case when the cooling rate in air is high, donor segregation is not expected to have occurred, although donor concentration is high. These results imply that, in the specimen where the donor distribution is initially homogeneous without segregation, donor segregation caused by the space charge potential can occur during the cooling process of the heat treatment in air.

In order to present direct evidence for the segregation related phenomena, compositional analysis was performed. Fig. 8 shows the microstructure of the 6 mol% Nb-2.6 mol% Mg-doped $BaTiO_3$ (net 0.8 mol% Nb) specimen that was sintered at 1300°C for 2 h in a reducing atmosphere ($PO_2 = 10^{-10}$ atm). The grain sizes range from 20–30 μm, and show a relatively homogeneous distribution. It was identified from EDS analysis that donor Nb distributes homogeneously at all points in the specimen. This specimen was heat-treated at 1400°C for 2 h in air with the cooling rate of 50°C/h to 900°C, then followed by furnace cooling (6Nb–2.6Mg–BT-50).

Fig. 9(a) and (b) shows the STEM/EDS results for the 6Nb–2.6Mg–BT-50 specimen at the grain boundary core and at a point 30 nm away. The intensity of the Nb peak at the grain boundary core is larger than that at a point 30 nm away from the grain boundary core. Among boundaries investigated, although some of them showed negligible donor segregation, many of them

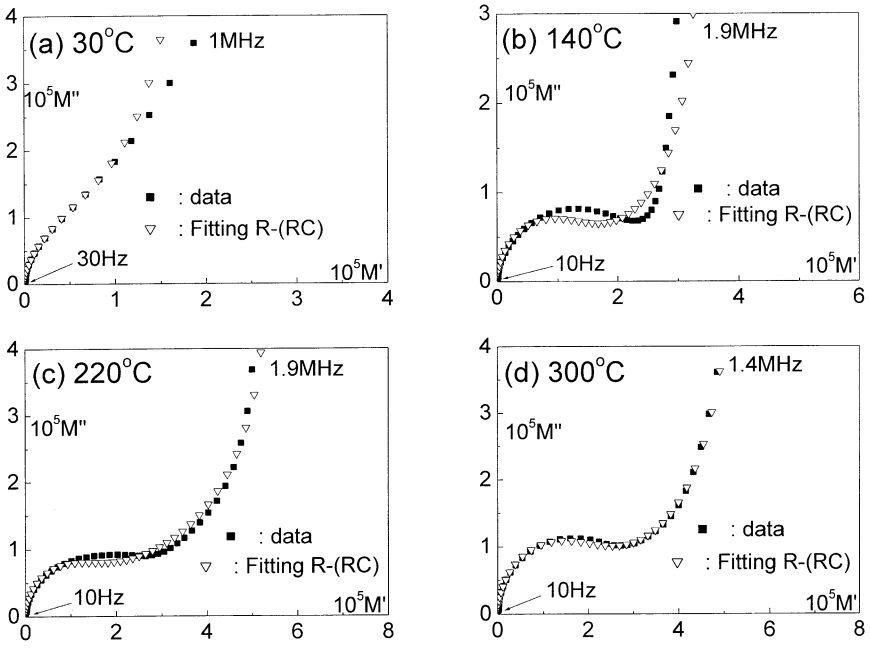

Fig. 7. Complex modulus plane plots of measured and fitted data for the 0.85Nb–BT-800 specimen at different temperatures: (a) 30°C, (b) 140°C, (c) 220°C, (d) 300°C.

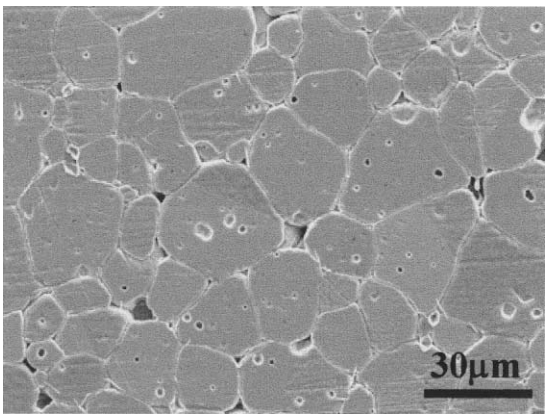

Fig. 8. Microstructure of the 6 mol% Nb–2.6 mol% Mg-doped $BaTiO_3$ (net 0.8 mol% Nb) specimen that was sintered at 1300°C for 2 h in a reducing atmosphere ($PO_2 = 10^{-10}$ atm).

showed donor segregation. Thus, donor segregation is confirmed. However, in the 6 mol% Nb–2.6 mol% Mg-doped $BaTiO_3$ specimen sintered only in a reducing atmosphere ($PO_2 = 10^{-10}$ atm) and not heat-treated in air, no difference in Nb peak intensities was observed between the grain boundary core and interior. This result directly implies that donor segregation has occurred during the cooling process after heat treatment in air, and that this segregation is caused by the space charge potential.

In order to provide somewhat more compelling evidence for the proposed relation between the electrical behavior and segregation of Nb, impedance analysis was performed for the 6 mol% Nb–2.6 mol% Mg-doped $BaTiO_3$ specimens. For the 6Nb–2.6Mg–BT-50 specimen, however, the resistivity of the specimen is too

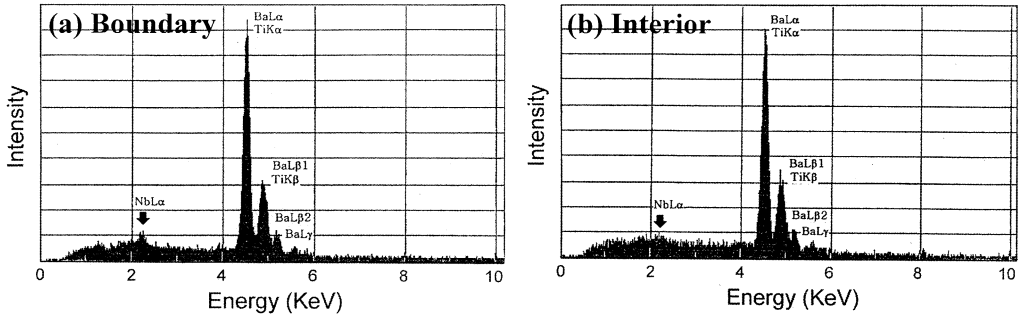

Fig. 9. STEM/EDS results for the 6Nb–2.6Mg–BT-50 specimen (a) at the grain boundary core, and (b) at a point 30 nm away from the grain boundary core.

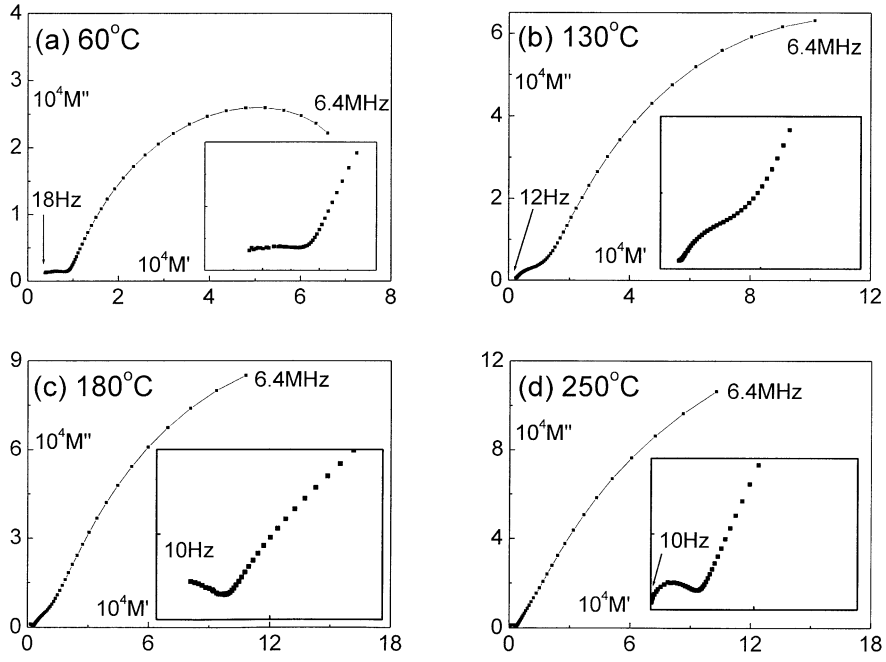

Fig. 10. Complex modulus plane plots of measured data at different temperatures for the 6 mol% Nb–2.6 mol% Mg-doped $BaTiO_3$ (net 0.8 mol% Nb) specimen that was sintered at 1300°C for 2 h in a reducing atmosphere ($PO_2 = 10^{-10}$ atm), and then heat-treated in air at 1400°C for 2 h with the cooling rate of 200°C: (a) 60°C, (b) 130°C, (c) 180°C, (d) 250°C.

high ($> 10^9$ Ωcm) in the measurement temperature range. Thus, proper impedance measurement and data analysis on this sample were impossible because of the limitations of the measurable range of an impedance analyzer. However, when the cooling rate of the 6Nb–2.6Mg–BT specimen was slightly increased and set to be 200°C/h, impedance data could narrowly be measured. 3RC terms could be identified in these data, and are shown in Fig. 10.

Fig. 10 shows the complex modulus plane plots of the measured data for the 6 mol% Nb–2.6 mol% Mg-doped $BaTiO_3$ specimen of which the cooling rate is 200°C/h. The behaviors of modulus data with the increase in temperature are almost the same as those for 0.85Nb–BT-160 specimen. As the temperatures increases, the behaviors of modules data change from three RC responses (60, 130 and 180°C data) to two RC responses (250°C data). Thus the proposed relation between the three RC responses and segregation of Nb can be confirmed.

In the same manner, donor segregation is expected to have occurred in the 0.85Nb–BT-160 specimen during the cooling process in air, and this phenomenon is associated with the third RC component in the impedance/modulus analysis.

3. Conclusions

Although the microstructures and R (resistivity)-T (temperature) characteristics are similar to each other, differences in the RC components of each specimen can occur if the net donor concentration of each specimen differs. The electrical modulus data of the specimen in which the net donor concentration is low, shows two RC components of the grain and grain boundary, although the cooling rate in air is low (0.1Nb–0.05Mn–BT-160 specimen). The modulus data of the specimen in which net donor concentration is high, show another third RC component when the cooling rate after heat treatment in air is low (0.85Nb–BT–160 specimen). The third RC component does not appear when the cooling rate in air is high (0.85Nb–BT-800 specimen). This RC component is associated with donor segregation. Therefore, it means that in the specimen where the donor distributes initially homogeneously without segregation, donor segregation can occur during the cooling process after heat treatment in air. This phenomenon corresponds to the space charge segregation theory for donor-doped $BaTiO_3$, which explains that space charge potential increases with decreasing temperature in air. The 6 mol% Nb–2.6 mol% Mg-doped $BaTiO_3$ specimen sintered in a reducing atmosphere shows negligible donor segregation although the net donor concentration is high (net 0.8 mol% Nb). However, when the specimen was again heat treated in air with a low cooling rate, donor segregation was detected from STEM / EDS analysis. This phenomenon can be direct evidence for space charge segregation during the cooling process in air for donor-doped $BaTiO_3$.

Acknowledgements

This work was supported in part by the Korea Science and Engineering Foundation through the Ceramic Processing Research Center (CPRC) at Hanyang University.

References

1. Chiang, Y. M. and Takagi, T., Grain-boundary chemistry of barium titanate and strontium titanate: I, high-temperature equilibrium space charge. *J. Am. Ceram. Soc.,* 1990, **73**(11), 3278–3285.
2. Horvath, G., Gerblinger, J., Meixner, H. and Giber, J., Segregation driving forces in perovskite titanates. *Sensors and Actuators,* 1996, **B32**, 93–99.
3. Desu, S. B. and Payne, D. A., Interfacial segregation in perovskites: II, experimental evidence. *J. Am. Ceram. Soc.,* 1990, **73**(11), 3398–3406.
4. Wilcox, N., Ravikumar, V., Rodrigues, R. P., Dravid, V. P., Vollmann, M., Waser, R., Soni, K. K. and Adriaens, A. G., Investigation of grain boundary segregation in acceptor and donor doped strontium titanate. *Solid State Ionics,* 1995, **75**, 127–136.
5. Peng, C. J. and Chiang, Y. M., Grain growth in donor-doped $SrTiO_3$. *J. Mater. Res.,* 1990, **5**(6), 1237–1245.
6. Woonbumroong, A., Brown, P. D. and Boothroyd, C. B., Grain-boundary segregation of Ho in $BaTiO_3$. *Inst. Phys. Conf. Ser. (Electron Microscopy and Analysis),* 1997, **153**(11), 507–510.
7. Jida, S., Suemasu, T. and Miki, T., Effect of microwave heating on $BaTiO_3$:Nb ceramics with positive temperature coefficient of resistivity. *J. Appl. Phys.,* 1999, **86**(4), 2089–2094.
8. Yoon, S. H., Lee, K. H. and Kim, H., Effect of acceptors on the segregation of donors in niobium-doped barium titanate positive temperature coefficient resistors. *J. Am. Ceram. Soc.,* 2000, **83**(10), 2463–2472.
9. Desu, S. B. and Payne, D. A., Interfacial segregation in perovskites: III microstructure and electrical properties. *J. Am. Ceram. Soc.,* 1990, **73**(11), 3407–3415.
10. Desu, S. B. and Payne, D. A., Interfacial segregation in perovskites:IV, internal boundary layer devices. *J. Am. Ceram. Soc.,* 1990, **73**(11), 3416–3421.
11. Fleig, J. and Maier, J., Finite-element calculation on the impedance of electroceramics with highly resistive grain boundaries: I, laterally inhomogeneous grain boundaries. *J. Am. Ceram. Soc.,* 1999, **82**(12), 3485–3493.
12. Hirose, N. and West, A. R., Impedance spectroscopy of undoped $BaTiO_3$ ceramics. *J. Am. Ceram. Soc.,* 1996, **79**(6), 1633–1641.